



Semnan University

Mechanics of Advanced Composite Structures

journal homepage: <https://MACS.journals.semnan.ac.ir>

Thermo–Elastic Stresses and Deformation Analysis of FG Rotating Hollow Spherical Body

L. Sondhi ^a, R. K. Sahu ^a, S. Bhowmick^b, A. K. Thawait^{c*}^a Department of Mechanical engineering, SSTC, SSGI, Bhilai, 490020, India^b Department of Mechanical engineering, NIT Raipur, Raipur, 492010, India^c Department of Mechanical engineering, IIT Bombay, Mumbai, 400076, India

KEYWORDS

Functionally graded material;
Hollow spherical body;
Axisymmetric body;
Analytical method;
Grading index.

ABSTRACT

In this paper, a generalized solution for 1-D steady-state thermo-mechanical analysis of the FG rotating hollow spherical body is presented. Deformation and stresses are calculated for a spherical body subjected to rotation, gravitation force, and uniform heat generation. Temperature distribution with uniform heat generation to the spherical body is assumed to vary along the radius. General thermal and mechanical boundary conditions at the inner surface and outer surfaces of the hollow spherical body are applied. Material properties are assumed as a power function of the radius with grading indices ranging from -2 to 3. Governing differential equation for the FG spherical body is developed and solved analytically. The obtained results are verified with benchmark results and are found to be in very good agreement. The result shows that deformation and stresses in the FG body are less compared to the homogeneous material body and the same is reported to decrease with increasing value of the grading parameter.

1. Introduction

Functionally graded materials (FGM) are a special group of heterogeneous composite materials with mechanical properties varying continuously from surface to surface at a macroscopic level. Thermo-mechanical stresses in the functionally graded thick spherical body are investigated by, R. Poultangari, M. R. Eslami, M.H. Babaei [1] wherein the performance of a thick hollow spherical body of functionally graded material under 1-dimensional steady state distributed temperature with a general thermo-mechanical type of boundary conditions is reported. Stresses and deformations in rotating functionally graded material pressurized thick hollow cylinder under thermal loading are investigated by, G. H. Rahimi and M. Zamani Nejad [2]. Effect of material gradient on stresses of the thick functionally graded spherical pressurized body using exponentially distributed material grading is reported by M Gharibi and M. Zamani Nejad [3]. A novel approach to stress analysis of pressurized functionally graded disc, cylinder, and spheres is established by N. Tutuncu, B.

Temel[4]. A functionally graded hollow cylindrical body under pressure and thermal loading conditions under the effect of material parameters on stresses and temperature distributions are presented by M. Gulgec and C. Evcı [5]. Elastic analysis of rotating spherical body, cylindrical body, and disc of variable thickness are reported by A. M. Zenkour [6]. Thermo-mechanical and thermo-elastic stresses were analysed in [7 - 10]. 2D thermal and elastic behaviour of functionally graded cylindrical body is studied and reported by Ghannad, Yaghoobi [11], wherein axisymmetric functionally graded cylindrical body subjected to external heat and pressure in the inner surface is reported. A spherical pressure vessel is designed and analysed using FEM by Afkar et al. [12]. Multi-scale hybrid disc resting on nonlinear elastic foundation under nonlinear frequency and extremely large oscillation is investigated by Ali Shariati et al. [13]. A shear deformation theory (refined quasi-3D theory) for the thermal and mechanical study of FG sandwich plates resting on two parameters elastic foundation is presented by Abdelkader Mahmoudi et al. [14].

* Corresponding author. Tel.: +91-8103180085.
E-mail address: amkthawait@gmail.com

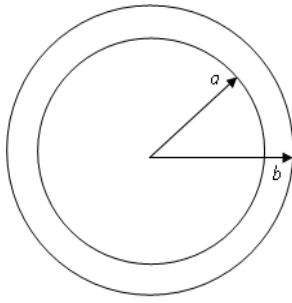


Fig. 1. Hollow spherical body

Nonlinear thermal-instability of electrically functionally graded GPLRC disc using GDQ method is investigated by M.S.H.Al-Furjan et al. [15]. Four variable quasi 3D HSDT is used for analytical modelling of vibration and bending of thick composite plates by Mokhtar Khiloun et al. [16]. Using a solid-state process, an application review of a functionally graded fabricated disk is reported by R. Madan and S. Bhowmick [17]. Limit elastic analysis of E-FG material-modeled rotating disc subjected to thermo-mechanical properties is studied by R. Madan et al. [18]. Thermal stresses induced due to internal heat generation (non-uniform heat) in FG hollow spherical bodies are reported by S. P. Pawar et al. [19]. Investigation of numerical, analytical, and experimental stress of spherical body having large volume is presented by Radovan Petrovic et al. [20].

In the present study, the deformation and changes in stresses of the functionally graded hollow spherical body are investigated. The problem is analytically solved using an in-house source code implementing the Navier equation for body force, rotation, and constant heat generation. The validation of the present study is carried out with existing literature. Corresponding to rotational speed, body force, and uniform heat generation in the spherical body, stress, and deformation are estimated. The existing results are reported in dimensionless form. There is a vast application of functionally graded spherical bodies such as submarine, pneumatic and hydraulic reservoirs, storage vessels, oil refineries, petrochemical plants, domestic hot water tanks, pressure reactors, autoclaves, etc.

2. Mathematical Formulation

Considering a rotating hollow spherical body made of functionally graded material, wherein the material properties of the body are assumed to be a power function of radius 'r'. Stress, strain, and displacement relations are given by [1]

$$\varepsilon_r = \frac{du}{dr} = \frac{1}{E(r)} [\sigma_r - 2\vartheta\sigma_t] + \alpha T(r) \quad (1)$$

$$\varepsilon_t = \frac{u}{r} = \frac{1}{E(r)} [\sigma_t(1-\vartheta) - \vartheta\sigma_r] + \alpha T(r) \quad (2)$$

Stress- strain relations [1] being:

$$\sigma_r = \frac{E(r)}{(1+\vartheta)(1-2\vartheta)} \left[\varepsilon_r(1-\vartheta) + 2\vartheta\varepsilon_t - (1+\vartheta)\alpha T(r) \right] \quad (3)$$

$$\sigma_t = \frac{E(r)}{(1+\vartheta)(1-2\vartheta)} \left[\vartheta\varepsilon_r + \varepsilon_t - (1+\vartheta)\alpha T(r) \right] \quad (4)$$

$T(r)$ is determined from the heat conduction equation in section 3. The equilibrium equation in the radial direction, including the inertia term and body force, is given by,

$$r \frac{d}{dr} \sigma_r + 2(\sigma_r - \sigma_t) + \rho \left(\omega^2 - \frac{g}{a} \right) r^2 = 0 \quad (5)$$

The power law is used to describe the material properties of a hollow spherical body which are given by [19],

$$E(r) = E_a (r)^{n_1} \quad (6)$$

$$\alpha(r) = \alpha_a (r)^{n_2} \quad (7)$$

$$k(r) = k_a (r)^{n_3} \quad (8)$$

$$\rho(r) = \rho_a (r)^{n_4} \quad (9)$$

$$q(r) = q_a (r)^{n_5} \quad (10)$$

Here, $E(r)$, $\alpha(r)$, $k(r)$, $\rho(r)$, $q(r)$ are modulus of elasticity, thermal expansion coefficient, thermal conduction coefficient, density, and heat generation at radius 'r' respectively. E_a , α_a , k_a , ρ_a , q_a are material properties as described above at radius 'a'

Using eq.(1) to (10), the Navier equation, in terms of displacement, is given by

$$\begin{aligned} & r \frac{d}{dr} \left[E\lambda \left\{ (1-\vartheta) \frac{du}{dr} + 2\vartheta \frac{u}{r} - (1+\vartheta)\alpha T \right\} \right] \\ & + E\lambda \left[\begin{aligned} & (1-\vartheta) \frac{du}{dr} + 2\vartheta \frac{u}{r} \\ & - (1+\vartheta)\alpha T \end{aligned} \right] \\ & - E\lambda \left[\vartheta \frac{du}{dr} + \frac{u}{r} - (1+\vartheta)\alpha T \right] \\ & + \rho \left(\omega^2 - \frac{g}{a} \right) r^2 = 0 \end{aligned} \quad (11)$$

in above eq. (11),

$$E = E(r), T = T(r), \alpha = \alpha(r), \rho = \rho(r) \quad (12)$$

$$\text{and } \lambda = \frac{1}{(1+\vartheta)(1-2\vartheta)}$$

3. Temperature Formulation

The 'one-dimensional heat conduction equation' with 'heat generation' in 'steady-state' condition in spherical coordinate is as follows [19].

$$\frac{1}{r^2} \frac{d}{dr} \left[r^2 k(r) \frac{dT(r)}{dr} \right] + q = 0 \tag{13}$$

Thermal boundary conditions[19] are:

$$T(r) = T(a) \quad \text{at} \quad r = a \quad \text{and} \tag{14}$$

$$T(r) = T(b) \quad \text{at} \quad r = b \tag{15}$$

where, $T(r)$ is the temperature at radius ' r ', $T(a)$ is the temperature at ' a ' and $T(b)$ is the temperature at ' b '.

Differentiating above eq. (13) of heat conduction, we get the Navier equation for temperature

$$A_1 r^2 T'' + B_1 r T' + C_1 T = \gamma_1 r^{n_5 - n_3 + 2} \tag{16}$$

where,

$$A_1 = k_a \tag{17}$$

$$B_1 = k_a (n_3 + 2) \tag{18}$$

$$C_1 = 0 \tag{19}$$

$$\gamma_1 = -q_a \tag{20}$$

$$P_3 = 0 \tag{21}$$

$$P_4 = \frac{A_1 - B_1}{A_1} = -n_3 - 1 \tag{22}$$

P_3 and P_4 are roots of the general solution of Eq. (16). After solving Eq. (16) analytically it gives,

$$T(r) = Q_3 + Q_4 r^{P_4} + \beta_1 r^{n_5 - n_3 + 2} \tag{23}$$

$$\frac{dT}{dr} = Q_4 P_4 r^{P_4 - 1} + \beta_1 (n_5 - n_3 + 2) r^{n_5 - n_3 + 1} \tag{24}$$

where,

$$\beta_1 = \frac{\gamma_1}{A_1 [(n_5 - n_3 + 2)(n_5 - n_3 + 1)] + B_1 [n_5 - n_3 + 2] + C_1}$$

Using the boundary conditions, the value of Q_3 and Q_4 yields

$$Q_4 = \frac{T_a - T_b}{a^{P_4} - b^{P_4}} - \frac{\beta_1 (a^{n_5 - n_3 + 2} - b^{n_5 - n_3 + 2})}{a^{P_4} - b^{P_4}} \tag{25}$$

$$Q_3 = T_a - \beta_1 a^{n_5 - n_3 + 2} - Q_4 a^{P_4} \tag{26}$$

4. Solutions of Displacement Equation

After solving the function $T(r)$ in above section 3, the value of $T(r)$ is put in eq. (11)

$$A r^2 u'' + B r u' + C u = U r^{n_2 + P_4 + 1} + V r^{n_2 - n_3 + n_5 + 3} + W r^{n_2 + 1} + S r^{n_4 - n_1 + 3} \tag{27}$$

where,

$$A = E_a \lambda (1 - \vartheta) \tag{28}$$

$$B = n_1 E_a \lambda (1 - \vartheta) + 2 E_a \lambda (1 - \vartheta) \tag{29}$$

$$C = 2 E_a \lambda \vartheta n_1 + 2 E_a \lambda \vartheta - 2 E_a \lambda \tag{30}$$

$$U = \frac{1}{(1 - 2\vartheta)} \left[\frac{E_a \alpha_a Q_4 P_4 + E_a \alpha_a Q_4 n_1}{E_a \alpha_a Q_4 n_2} \right] \tag{31}$$

$$V = \frac{\beta_1 E_a \alpha_a}{(1 - 2\vartheta)} [n_5 - n_3 + n_1 + n_2 + 2] \tag{32}$$

$$W = \frac{Q_3 E_a \alpha_a}{(1 - 2\vartheta)} [n_1 + n_2] \tag{33}$$

$$S = -\rho \left[\omega^2 - \left(\frac{g}{a} \right) \right] \tag{34}$$

Equation (27) is the Navier equation, which is a non-homogeneous Euler differential equation. Assuming general solution, u_g as

$$u_g(r) = Q r^P \tag{35}$$

Substituting the eq. (35) in homogeneous form of eq. (27)

$$A P^2 + (B - A) P + C = 0 \tag{36}$$

The above eq. (36) has two real roots P_1 And P_2 As,

$$P_{1,2} = \frac{(A - B) \pm \sqrt{(B - A)^2 - 4AC}}{2A} \tag{37}$$

Now, the general solution is

$$u_g(r) = Q_1 r^{P_1} + Q_2 r^{P_2} \tag{38}$$

Assuming the particular solution $u_p(r)$ in the form,

$$u_p(r) = I r^{n_2 + P_4 + 1} + J r^{n_2 - n_3 + n_5 + 3} + L r^{n_2 + 1} + M r^{n_4 - n_1 + 3} \tag{39}$$

Substituting the above Eq. (39) in eq. (27), we get,

$$\begin{aligned}
 & [A(n_2 + P_4 + 1)(n_2 + P_4) + B(n_2 + P_4 + 1) + C] I r^{n_2 + P_4 + 1} \\
 & + \left[\frac{A(n_2 - n_3 + n_5 + 3)(n_2 - n_3 + n_5 + 2) + B(n_2 - n_3 + n_5 + 3) + C}{J} \right] J r^{n_2 - n_3 + n_5 + 3} \\
 & + [A(n_2 + 1)n_2 + B(n_2 + 1) + C] L r^{n_2 + 1} \quad (40) \\
 & + [A(n_4 - n_1 + 3)(n_4 - n_1 + 2) + B(n_4 - n_1 + 3) + C] M r^{n_4 - n_1 + 3} \\
 & = U r^{n_2 + P_4 + 1} + V r^{n_2 - n_3 + n_5 + 3} + W r^{n_2 + 1} + S r^{n_4 - n_1 + 3}
 \end{aligned}$$

Equating the coefficients of identical power in above eq. (40), we have

$$I = \frac{U}{A[(n_2 + P_4 + 1)(n_2 + P_4)] + B[n_2 + P_4 + 1] + C} \quad (41)$$

$$J = \frac{V}{A[(n_2 - n_3 + n_5 + 3)(n_2 - n_3 + n_5 + 2)] + B[(n_2 - n_3 + n_5 + 3)] + C} \quad (42)$$

$$L = \frac{W}{A[(n_2 + 1)(n_2)] + B[(n_2 + 1)] + C} \quad (43)$$

$$M = \frac{S}{A[(n_4 - n_1 + 3)(n_4 - n_1 + 2)] + B[(n_4 - n_1 + 3)] + C} \quad (44)$$

Complete solution for displacement function $u(r)$ is given by,

$$u(r) = u_g(r) + u_p(r) \quad (45)$$

Thus

$$\begin{aligned}
 u(r) = & Q_1 r^{P_1} + Q_2 r^{P_2} + I r^{n_2 + P_4 + 1} + J r^{n_2 - n_3 + n_5 + 3} \\
 & + L r^{n_2 + 1} + M r^{n_4 - n_1 + 3}
 \end{aligned} \quad (46)$$

Substituting eq. (46) in eq. (1) to (2), the strains and stresses are obtained as,

$$\begin{aligned}
 \epsilon_r = & Q_1 p_1 r^{P_1 - 1} + Q_2 p_2 r^{P_2 - 1} + I(n_2 + P_4 + 1) r^{n_2 + P_4} \\
 & + J(n_2 - n_3 + n_5 + 3) r^{n_2 - n_3 + n_5 + 2} + L(n_2 + 1) r^{n_2} \\
 & + M(n_4 - n_1 + 3) r^{n_4 - n_1 + 2}
 \end{aligned} \quad (47)$$

$$\begin{aligned}
 \epsilon_t = & Q_1 r^{P_1 - 1} + Q_2 r^{P_2 - 1} + I r^{n_2 + P_4} + J r^{n_2 - n_3 + n_5 + 2} \\
 & + L r^{n_2} + M r^{n_4 - n_1 + 2}
 \end{aligned} \quad (48)$$

$$\sigma_r = E\lambda \left[\begin{aligned} & Q_1 \{ (1-\vartheta)P_1 + 2\vartheta \} r^{n_1 + P_1 - 1} + Q_2 \{ (1-\vartheta)P_2 + 2\vartheta \} \\ & r^{n_1 + P_2 - 1} + I r^{n_1 + n_2 + P_4} [(1-\vartheta)(n_2 + P_4 + 1) + 2\vartheta] + \\ & J r^{n_1 + n_2 - n_3 + n_5 + 2} [(1-\vartheta)(n_2 - n_3 + n_5 + 3) + 2\vartheta] + \\ & L r^{n_1 + n_2} [(1-\vartheta)(n_2 + 1) + 2\vartheta] + \\ & M r^{n_1 + n_2} [(1-\vartheta)(n_4 - n_1 + 3) + 2\vartheta] - \\ & (1-\vartheta)\alpha [Q_3 a^{n_1 + n_2} + Q_4 r^{n_1 + n_2 + P_4} + \beta_1 r^{n_1 + n_2 + n_3 - n_5 + 2}] \end{aligned} \right] \quad (49)$$

To determine the constants Q_1 and Q_2 , the boundary conditions for stress profile are used. Considering the mechanical boundary conditions in the radius 'a' and outer radius 'b' [1]

$$\sigma_r(a) = -p_a \quad \text{and} \quad \sigma_r(b) = -p_b \quad (50)$$

Substituting the above eq. (50) in eq. (49), the integration constants become:

$$Q_1 = \frac{\phi_{22} X - \phi_{12} Y}{\phi_{11} \phi_{22} - \phi_{12} \phi_{21}} \quad (51)$$

$$Q_2 = \frac{\phi_{11} Y - \phi_{21} X}{\phi_{11} \phi_{22} - \phi_{12} \phi_{21}} \quad (52)$$

where,

$$\phi_{11} = E_a \lambda [P_1(1-\nu) + 2\nu] a^{n_1 + P_1 - 1} \quad (53)$$

$$\phi_{12} = E_a \lambda [P_2(1-\nu) + 2\nu] a^{n_1 + P_2 - 1} \quad (54)$$

$$\phi_{21} = E_a \lambda [P_1(1-\nu) + 2\nu] b^{n_1 + P_1 - 1} \quad (55)$$

$$\phi_{22} = E_a \lambda [P_2(1-\nu) + 2\nu] b^{n_1 + P_2 - 1} \quad (56)$$

$$X = -p_a - Z(a), \quad Y = -p_b - Z(b) \quad (57)$$

$$\begin{aligned}
 Z(a) = & E_a \lambda a^{n_1 + n_2 + P_4} [(1-\vartheta)(n_2 + P_4 + 1) + 2\vartheta] + \\
 & J a^{n_1 + n_2 - n_3 + n_5 + 2} [(1-\vartheta)(n_2 - n_3 + n_5 + 3) + 2\vartheta] + \\
 & L a^{n_1 + n_2} [(1-\vartheta)(n_2 + 1) + 2\vartheta] + M a^{n_1 + n_2} [(1-\vartheta)(n_4 - n_1 + 3) \\
 & + 2\vartheta] - (1-\vartheta)\alpha [Q_3 a^{n_1 + n_2} + Q_4 a^{n_1 + n_2 + P_4} + \beta_1 a^{n_1 + n_2 + n_3 - n_5 + 2}]
 \end{aligned} \quad (58)$$

$$\begin{aligned}
 Z(b) = & E_a \lambda b^{n_1 + n_2 + P_4} [(1-\vartheta)(n_2 + P_4 + 1) + 2\vartheta] + \\
 & J b^{n_1 + n_2 - n_3 + n_5 + 2} [(1-\vartheta)(n_2 - n_3 + n_5 + 3) + 2\vartheta] + L b^{n_1 + n_2} \\
 & [(1-\vartheta)(n_2 + 1) + 2\vartheta] + M b^{n_1 + n_2} [(1-\vartheta)(n_4 - n_1 + 3) + 2\vartheta] \\
 & - (1-\vartheta)\alpha [Q_3 b^{n_1 + n_2} + Q_4 b^{n_1 + n_2 + P_4} + \beta_1 b^{n_1 + n_2 + n_3 - n_5 + 2}]
 \end{aligned} \quad (59)$$

5. Result and Discussion

FG Spherical Body Subjected to Internal Pressure and Temperature

The numerical values of different parameters considered in the work are as follows: the inner and outer radius of the hollow spherical body are $a = 1$ m, $b = 1.2$ m, Poisson's ratio $\nu = 0.3$ since it is considered that material properties are in accordance with eq. (6) to (10). The internal properties of the hollow spherical body are as follows: modulus of elasticity $E_a = 200$ GPa, thermal coefficient of expansion $\alpha_a = 1.2 \times 10^{-6}$ per $^\circ\text{C}$, thermal conduction coefficient $k_a = 15$

W/mK, Density $\rho_a = 7800 \text{ kg/m}^3$, Heat generation $q = 50 \times 10^3 \text{ kJ/m}^3$ and Gravity $g = 9.81 \text{ m/s}^2$ Rotation $\omega = 50 \text{ rad/s}$. Thermal boundary conditions are taken as $T(a) = 10 \text{ }^\circ\text{C}$ and $T(b) = 0 \text{ }^\circ\text{C}$. Mechanical Boundary conditions are taken as internal pressure of 50 MPa and External pressure = 0; material grading indices 'n' are chosen as -2 to 3 and $n_1 = n_2 = n_3 = n_4$ are identical but, $n_5 = 0$ [1].

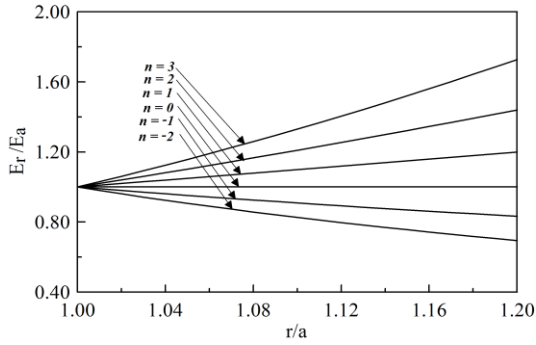


Fig. 2. Variation of elasticity modulus along the radius

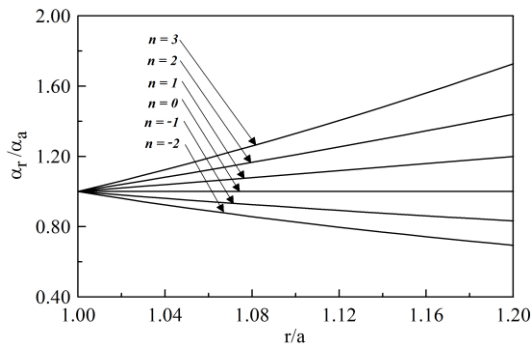


Fig. 3. Radial variation of thermal expansion coefficient

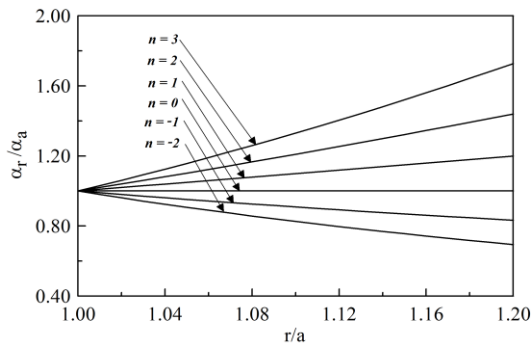


Fig. 4. Variation of density along the radius

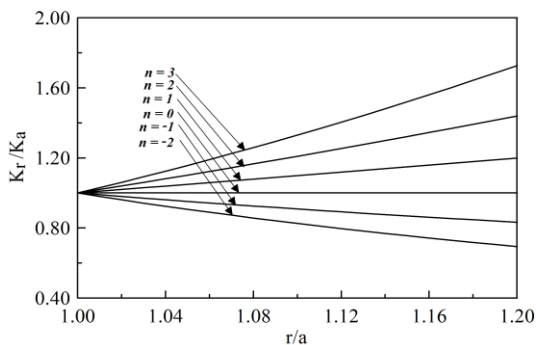


Fig. 5. Radial variation of thermal conduction coefficient

The above graphs show the material property variation wherein Fig. 2 is for elastic modulus, Fig. 3 is for thermal expansion coefficient, Fig. 4 is for material density and Fig. 5 for thermal conduction coefficient for $n = -2$ to 3.

For $n = 1$ to 3 the value of material properties are in increasing order from radius a to radius b while for $n = -1$ to -2 the value of material properties are in decreasing order from radius a to radius b .

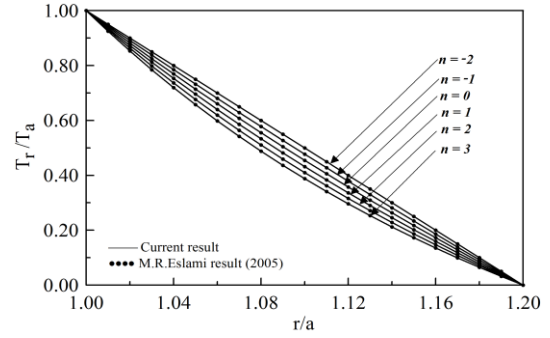


Fig. 6. Variation of temperature along the radius

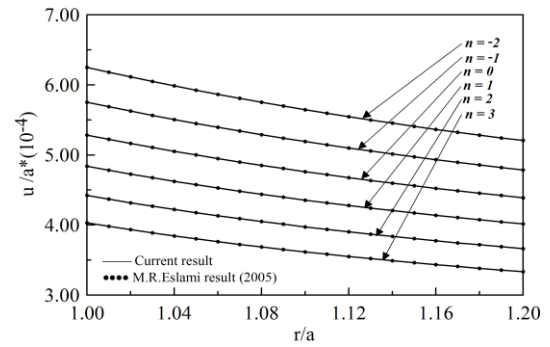


Fig. 7. Variation of radial displacement

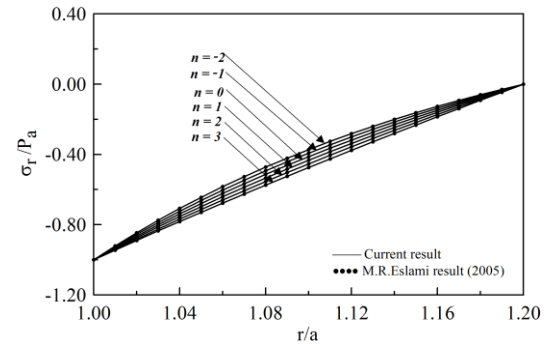


Fig. 8. Variation of radial stress

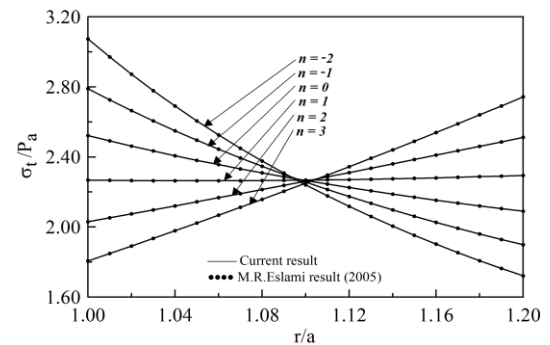


Fig. 9. Variation of tangential stress

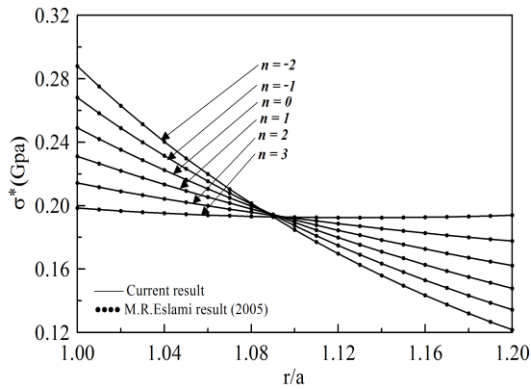


Fig. 10. Variation of von-Mises stress for $b/a = 1.2$

Graphs plotted in Fig. 6 to Fig. 10 show the validation of the present study, which are found to be in good agreement with reference [1] for grading indices ranging from $n = -2$ to 3. It is shown in Fig. 6 that the temperature varies inversely with the radius and grading indices, too. In Fig. 7, radial displacement is plotted and is observed to be inversely proportional to the grading index ' n '. In Fig. 8, radial stresses are plotted and are reported to vary directly with radius. Fig. 9 reports tangential stress that is decreasing radially outward for $n < 1$, but increasing outward for $n > 1$ and constant throughout the thickness for $n = 1$. The von-Mises stress is investigated and plotted in Fig. 10. It is clearly observed from the graph that Von-Mises stress is inversely proportional to the grading index up to $r/a = 1.10$ beyond which there is a reversal in variation.

Case 1: Rotating FG Spherical Body

Herein, a functionally graded rotating hollow spherical body is investigated under the effect of rotation in a hollow spherical body. Fig. 11 reports the temperature distribution for grading indices ranging from $n = -2$ to 3 and it is observed that temperature varies inversely to the grading index for FG rotating hollow sphere.

In Fig. 12, it is shown that radial displacement is inversely proportional to the grading index ' n '. Fig. 13 shows the distribution of radial stress that is directly proportional to the radius i.e. temperature at outer radius is higher than inner radius but radial stress is inversely proportional to the grading index ' n '. Fig. 14 reports that tangential stress is decreasing radially outward for $n < 1$, but increasing outward for $n > 1$ and constant throughout the thickness for $n = 1$. The von-Mises stress is investigated in Fig. 15. It is evident from the figure that Von-Mises stress is inversely proportional to the grading index up to $r/a = 1.08$ (approx.) beyond which the von-Mises stress becomes directly proportional to the grading index.

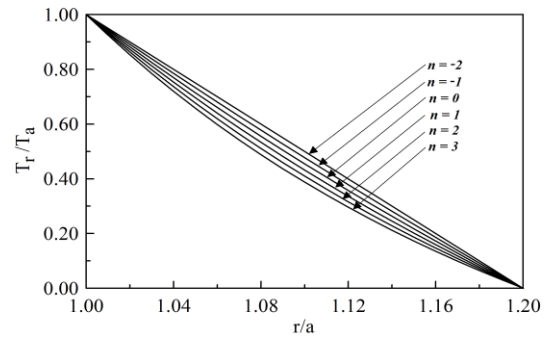


Fig. 11. Variation of temperature

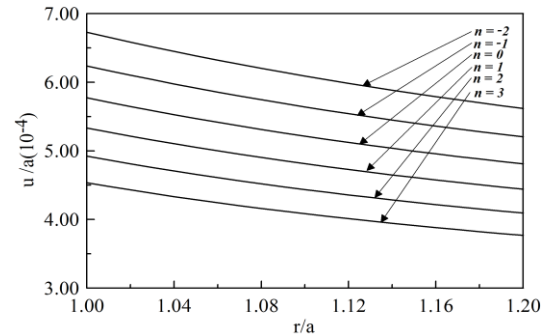


Fig. 12. Variation of radial displacement

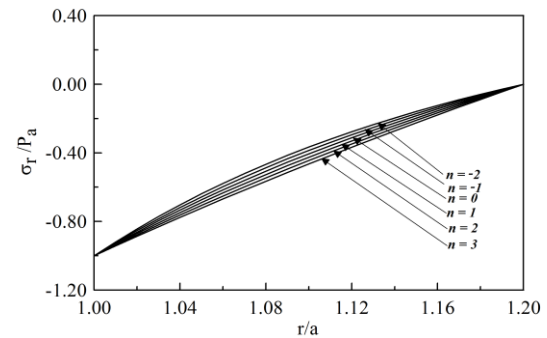


Fig. 13. Variation of radial stress

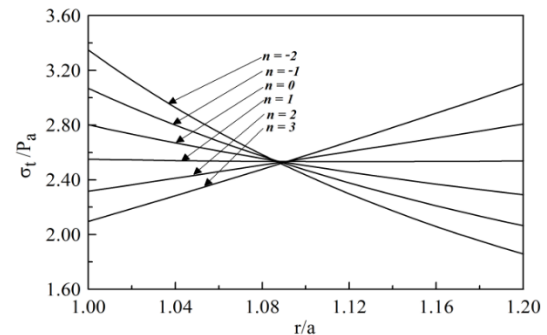


Fig. 14. Variation of tangential stress

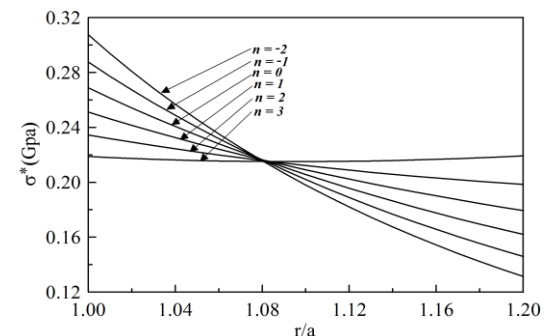


Fig. 15. Variation of von-Mises stress

Case 2: FG Hollow Spherical Body Subjected to Gravitational Force

The effect of gravitational force on the functionally graded hollow spherical body is investigated and reported in this sub-section. The distribution of temperature for different grading indexes 'n' is shown in Fig. 16. Similar to case 1, the temperature distribution is inversely proportional to the radius of the hollow spherical body and grading index too. The distribution of radial displacement shown in Fig. 17 is inversely proportional to the radius of the hollow spherical body and grading index too. The radial stress distribution is shown in Fig. 18 wherein it is observed to be directly proportional to the radius but inversely proportional to the grading index of the hollow spherical body as in the previous case. The tangential stress distribution is plotted in Fig. 19 wherein it is observed to decrease along the radius for $n < 1$, but increases outward for $n > 1$ and remains constant throughout the thickness for $n = 1$ similar to case 1.

The variation in Von-Mises stress is plotted in Fig. 20. It is clearly observed from the graph that Von-Mises stress is inversely proportional to the grading index up to $r/a = 1.09$ (approx.) beyond which there is a reversal in variation.

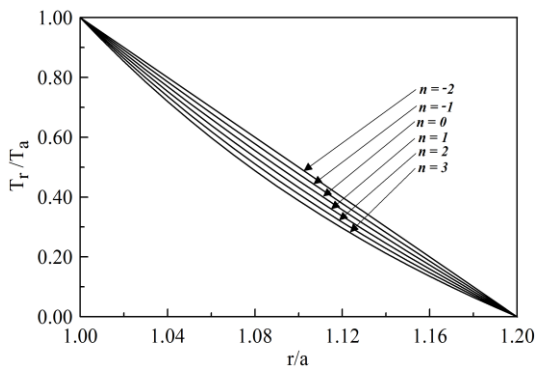


Fig. 16. Variation of temperature

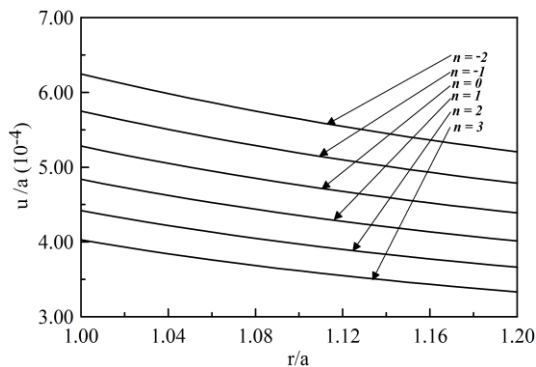


Fig. 17. Variation of displacement

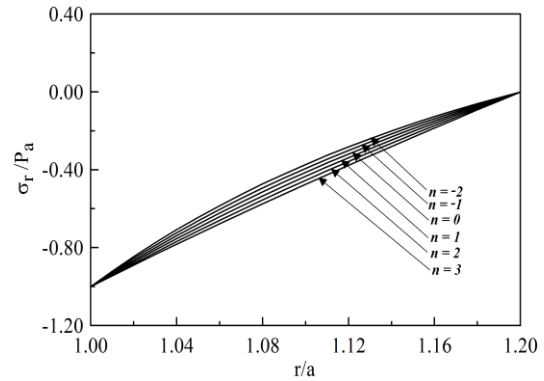


Fig. 18. Variation of radial stress

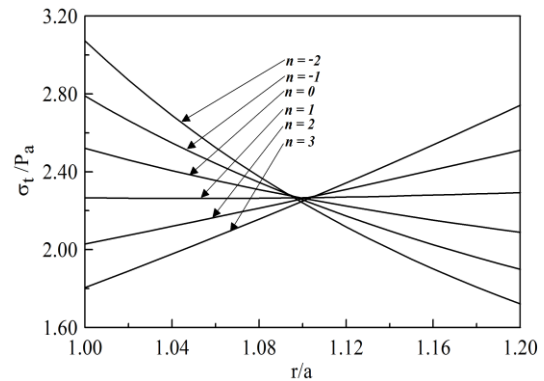


Fig. 19. Variation of tangential stress

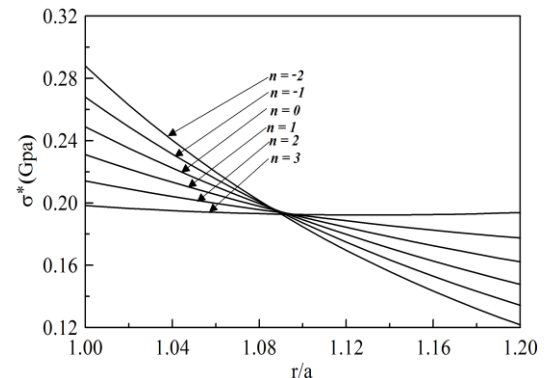


Fig. 20. Variation of von-Mises stress

Case 3: FG Spherical Body Subjected to Constant Heat Generation

In this section, the effect of constant heat generation on the displacement and stresses is investigated for the hollow spherical body. The results are reported in a similar sequence of graphs as mentioned for the remaining cases. (Fig. 21 – Fig. 25). The reversal in the variation of Von-Mises stress is observed to occur at $r/a = 1.09$ (approx.) as shown in Fig. 25.

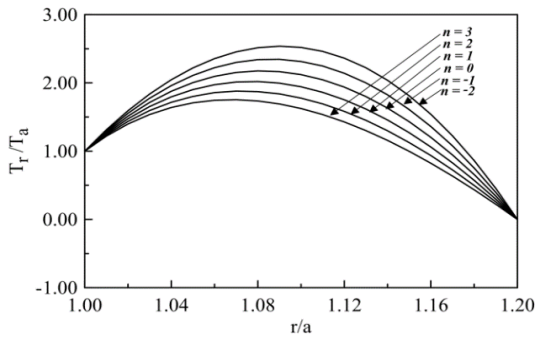


Fig. 21. Variation of temperature

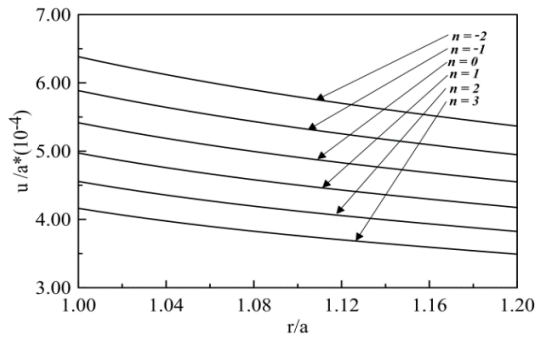


Fig. 22. Variation of displacement

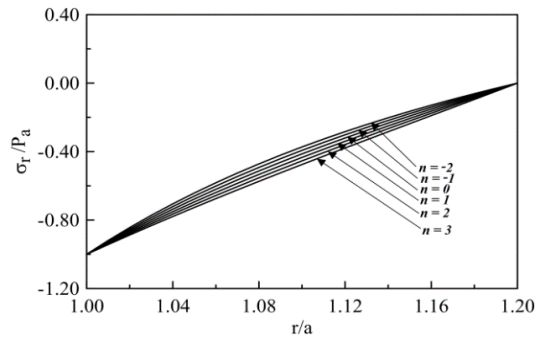


Fig. 23. Variation of radial stress

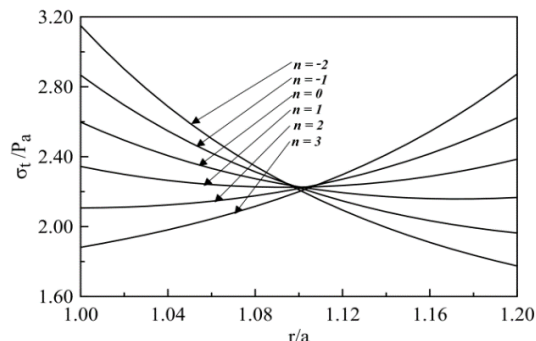


Fig. 24. Variation of tangential stress

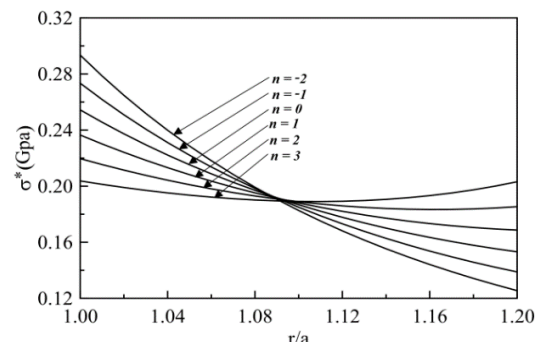


Fig. 25. Variation of von-Mises stress

Case 4: FG Spherical Body Subjected to Gravitational Force and Rotation

Herein, the effect of gravitation and rotational force on displacement and stresses of the functionally graded hollow spherical body is investigated and the results are reported in Fig. 26 - Fig. 30 in a similar sequence of graphs.

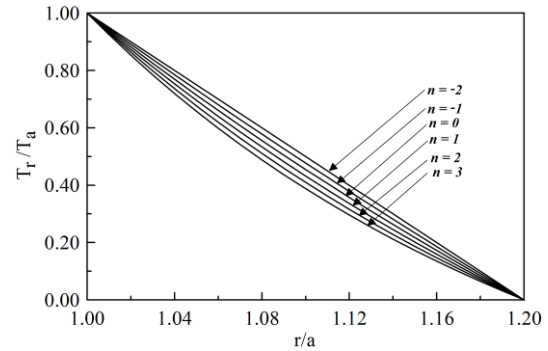


Fig. 26. Variation of temperature

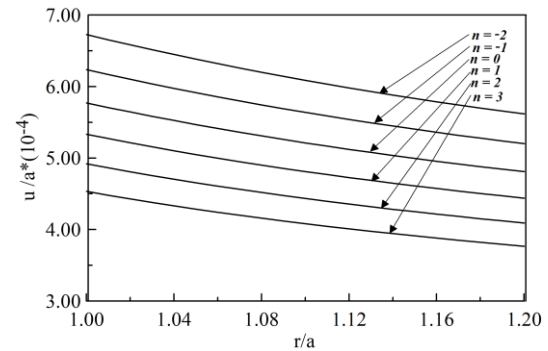


Fig. 27. Variation of displacement

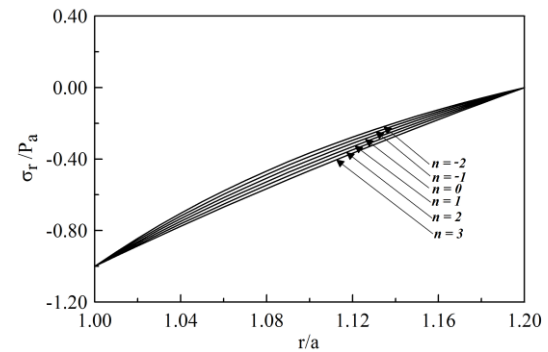


Fig. 28. Variation of radial stress

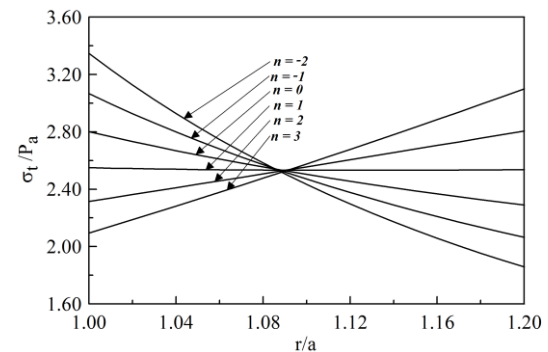


Fig. 29. Variation of tangential stress

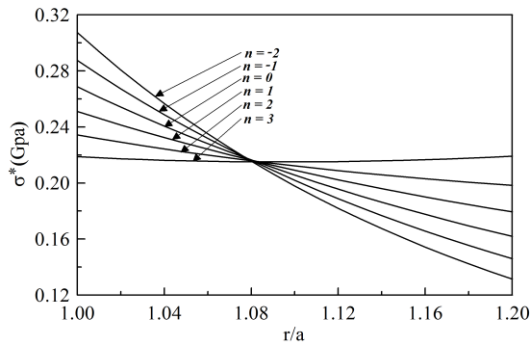


Fig. 30. Variation of von-Mises stress

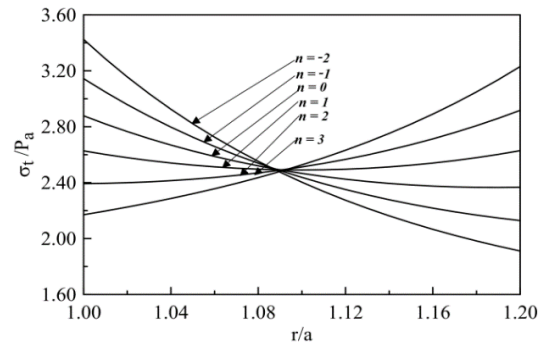


Fig. 34. Variation of tangential stress

Case 5: Rotating Spherical Body with Constant Heat Generation

The displacement and stresses for a functionally graded hollow spherical body under the effect of centrifugal loading and constant heat generation are reported herein (Fig. 31-Fig.35).

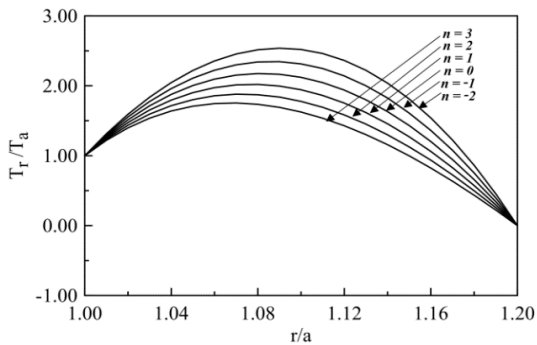


Fig. 31. Variation of temperature

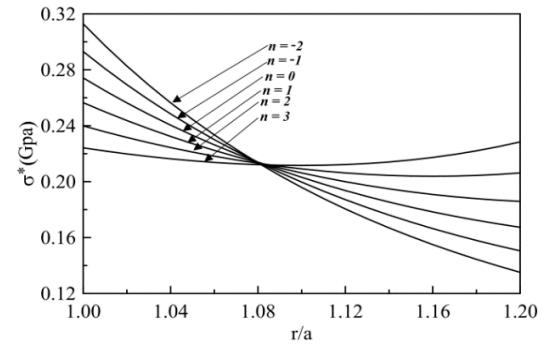


Fig. 35. Variation of von-Mises stress

Case 6: FG Spherical Body Subjected to Constant Heat Generation and Gravitation

Herein, the effect of constant heat generation and gravitation on the stresses and displacement field of the hollow spherical body is investigated and reported (Fig. 36-Fig. 40).

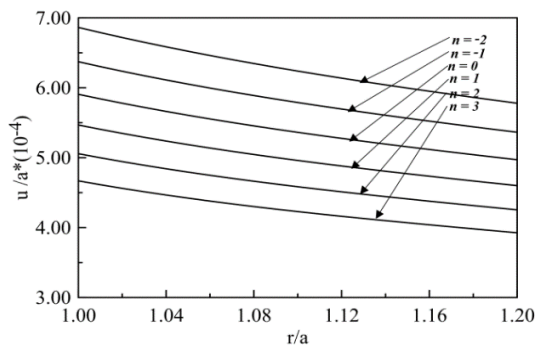


Fig. 32. Variation of displacement

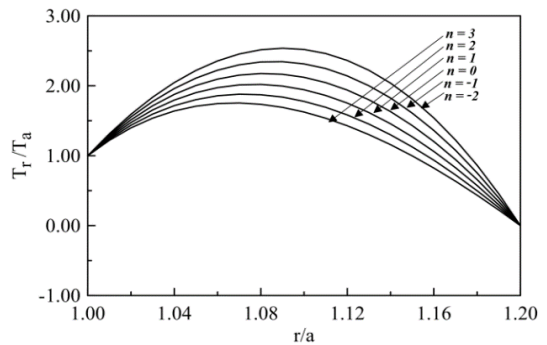


Fig. 36. Variation of temperature

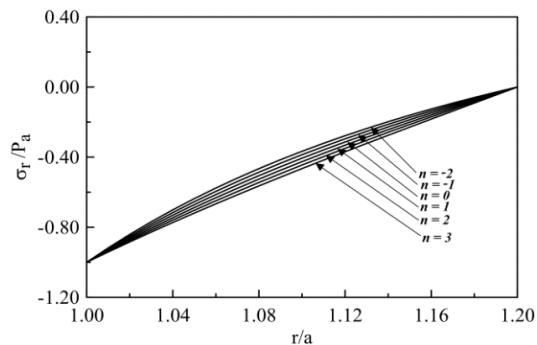


Fig. 33. Variation of radial stress

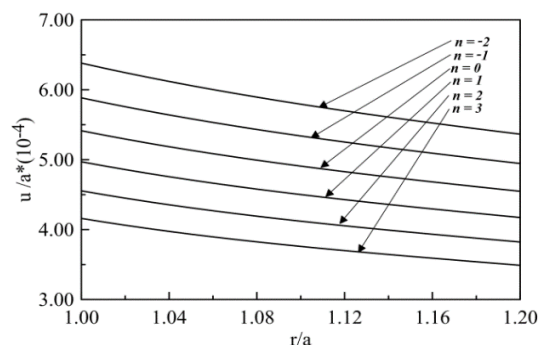


Fig. 37. Variation of displacement

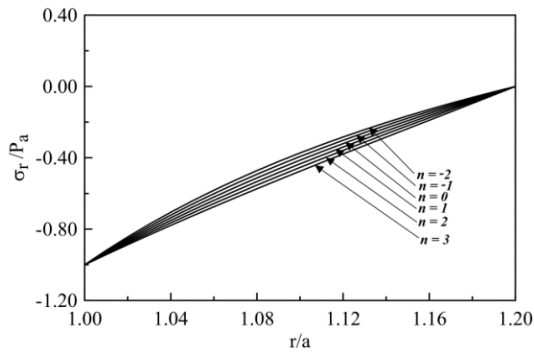


Fig. 38. Variation of radial stress

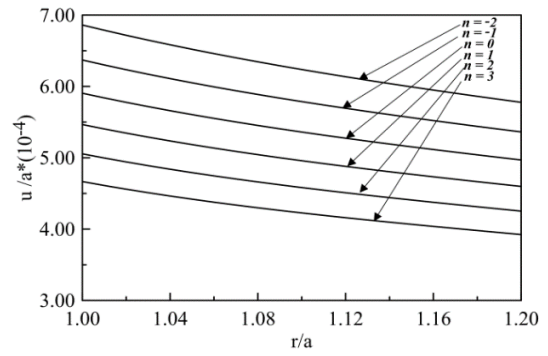


Fig. 42. Variation of displacement

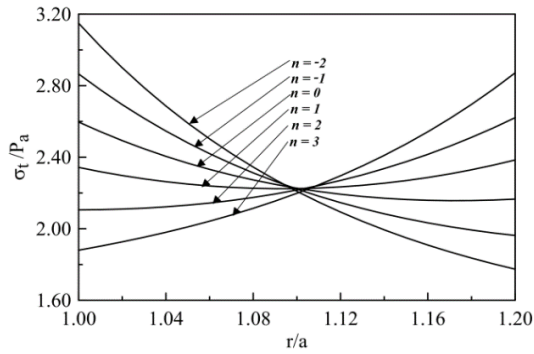


Fig. 39. Variation of tangential stress

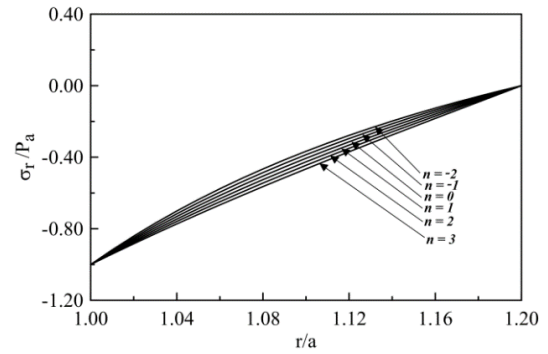


Fig. 43. Variation of radial stress

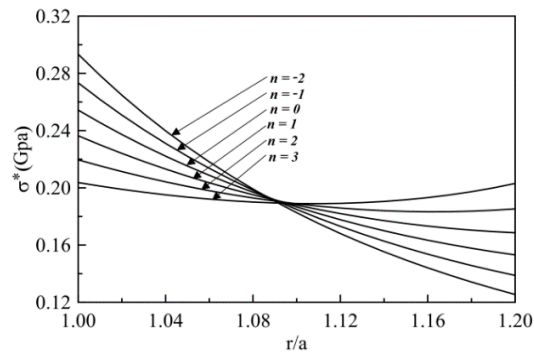


Fig. 40. Variation of von-Mises stress

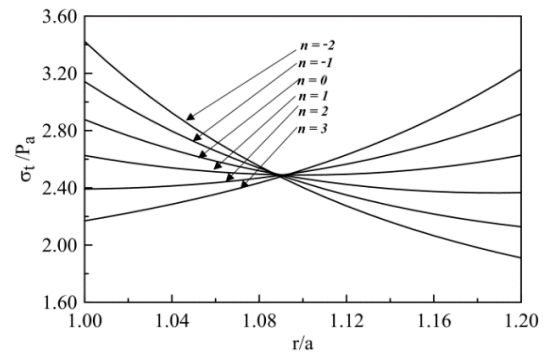


Fig. 44. Variation of tangential stress

Case 7: Rotating FG Hollow Sphere Under Gravitation and Constant Heat Generation

The stresses and displacements of a rotating hollow spherical body with gravitation and constant heat generation are investigated and reported in Fig. 41-Fig. 45.

The variation of Von-Mises stresses for various loading conditions as reported in cases 1-7 in FG hollow spherical body for $b/a = 1.2$ is reported in Fig. 15, Fig. 20, Fig. 25, Fig. 30, Fig. 35, Fig. 40, Fig. 45 with respect to grading indices ranging from $n=-2$ to 3.

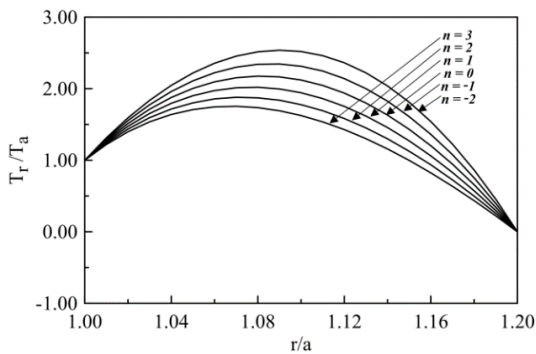


Fig. 41. Variation of temperature

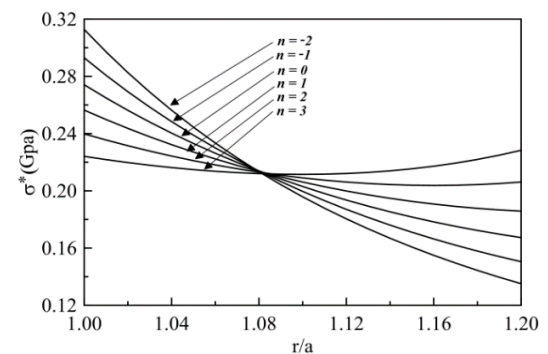


Fig. 45. Variation of von-Mises stress

It is evident that for a hollow sphere subjected to rotation in presence of other gravitation and/or constant heat generation, the distribution of Von-Mises stresses along the radial direction attains maximum value as shown in Fig. 35 and Fig. 45. The von-Mises stress distribution is lowest for case 2 as shown in Fig. 20.

It has been also observed that, for r/a in the range of 1.08 to 1.1(approx.), the reversal of the gradient of Von-Mises stresses is obtained in relation to grading indices, i.e. for $r/a < 1.08$ (approx.) the von-Mises stress is inversely proportional to the grading index and for $r/a > 1.1$ (approx.) the von-Mises stress is directly proportional to the grading index. The Von-Mises stress at $b/a = 1.08$, corresponding to grading indices and different loading conditions, is reported in Table 1.

Table 1: For cases 1-7 the Von-Mises stresses (σ^*) at $b/a = 1.08$

Cases	Grading index					
	-2	-1	0	1	2	3
Case 1	0.21	0.21	0.21	0.21	0.21	0.21
Case 2	0.20	0.20	0.19	0.19	0.19	0.19
Case 3	0.19	0.19	0.19	0.19	0.19	0.19
Case 4	0.21	0.21	0.21	0.21	0.21	0.21
Case 5	0.21	0.21	0.21	0.21	0.21	0.21
Case 6	0.19	0.19	0.19	0.19	0.19	0.19
Case 7	0.21	0.21	0.21	0.21	0.21	0.21

6. Conclusion

The present study reports the exact solution for elastic and thermoelastic deformation and stresses of the FG rotating spherical body. Power law grading of material properties along the radial direction has been considered in the formulation. Stresses and displacement are obtained through the direct solution of the Navier equation and the effect due to grading index, rotational, gravitation force, and constant heat generation are investigated for the hollow spherical body.

- The effect of grading index is investigated for hollow spherical body and it is observed that grading index is directly proportional to the strength of the hollow spherical body.
- The effect of grading index on the displacement of FG hollow spherical body has been investigated and it is observed that the grading index is inversely proportional to the radial displacement.

- Due to the nature of the loading and boundary conditions, the displacement field is observed to decrease along the radius towards the periphery of the hollow sphere.
- Radial stresses are found to vary inversely with the variation of grading indices at any radial location.
- For $n < 1$, the tangential stress is inversely proportional to the radius, while for $n > 1$, the tangential stress is directly proportional to the radius and for $n = 1$, tangential stress is uniform along the radius.
- The von-Mises stress distribution is plotted along the radius to study the overall stress distribution. The von-Mises stress is almost uniform along the radius for $n = 3$. This is an interesting observation as this leads to the design of a functionally graded hollow sphere having uniform strength. In other words, it may be observed that the grading index of $n = 3$ in power law grading leads to the design of an FG hollow sphere of uniform strength.
- The Von-Mises stresses are inversely proportional to the grading index until a critical value of ' b/a ' is reached. Beyond this, the variation of Von-Mises stresses undergoes a reversal in relation to the grading index.

Nomenclature

a	inner radius of the hollow sphere
b	outer radius of the hollow sphere
u	displacement in the radial direction
$\epsilon_i (i = r, t)$	strain tensor
$\sigma_i (i = r, t)$	stress tensor
α	thermal expansion coefficient
ρ	material density
ω	rotation
g	gravitational force
$n_j (j = 1 \text{ to } 5)$	grading index

References

- [1] Eslami, M.R., Babaei, M.H. and Poultangari, R., 2005. Thermal and mechanical stresses in a functionally graded thick sphere. *International Journal of Pressure Vessels and Piping*, 82(7), pp.522-527.
- [2] Nejad, M.Z. and Rahimi, G.H., 2009. Deformations and stresses in rotating FGM pressurized thick hollow cylinder under

- thermal load. *Scientific Research and Essays*, 4(3), pp.131-140.
- [3] Nejad, M. and Gharibi, M., 2014. Effect of material gradient on stresses of thick FGM spherical pressure vessels with exponentially-varying properties. *Journal of Advanced Materials and Processing*, 2(3), pp.39-46.
- [4] Tutuncu, N. and Temel, B., 2009. A novel approach to stress analysis of pressurized FGM cylinders, disks and spheres. *Composite structures*, 91(3), pp.385-390.
- [5] Evci, C. and Gülgeç, M., 2018. Functionally graded hollow cylinder under pressure and thermal loading: Effect of material parameters on stress and temperature distributions. *International Journal of Engineering Science*, 123, pp.92-108.
- [6] Zenkour, A.M., 2010. Rotating Variable-Thickness Inhomogeneous Cylinders: Part I-Analytical Elastic Solutions. *Applied Mathematics*, 1(6), p.481.
- [7] Xin, L., Dui, G., Yang, S. and Zhou, D., 2015. Solutions for behavior of a functionally graded thick-walled tube subjected to mechanical and thermal loads. *International Journal of Mechanical Sciences*, 98, pp.70-79.
- [8] Sadeghian, M. and Toussi, H.E., 2011. Axisymmetric yielding of functionally graded spherical vessel under thermo-mechanical loading. *Computational Materials Science*, 50(3), pp.975-981.
- [9] Boroujerdy, M.S. and Eslami, M.R., 2014. Axisymmetric snap-through behavior of Piezo-FGM shallow clamped spherical shells under thermo-electro-mechanical loading. *International Journal of Pressure Vessels and Piping*, 120, pp.19-26.
- [10] Ranjbar, J. and Alibeigloo, A., 2016. Response of functionally graded spherical shell to thermo-mechanical shock. *Aerospace Science and Technology*, 51, pp.61-69.
- [11] Ghannad, M. and Yaghoobi, M.P., 2017. 2D thermo elastic behavior of a FG cylinder under thermomechanical loads using a first order temperature theory. *International Journal of Pressure Vessels and Piping*, 149, pp.75-92.
- [12] Afkar, A., Camari, M.N. and Paykani, A., 2014. Design and analysis of a spherical pressure vessel using finite element method. *World journal of modelling and simulation*, 10(2), pp.126-135.
- [13] Shariati, A., Ghabussi, A., Habibi, M., Safarpour, H., Safarpour, M., Tounsi, A. and Safa, M., 2020. Extremely large oscillation and nonlinear frequency of a multi-scale hybrid disk resting on nonlinear elastic foundation. *Thin-Walled Structures*, 154, p.106840.
- [14] Mahmoudi, A., Benyoucef, S., Tounsi, A., Benachour, A., Adda Bedia, E.A. and Mahmoud, S.R., 2019. A refined quasi-3D shear deformation theory for thermo-mechanical behavior of functionally graded sandwich plates on elastic foundations. *Journal of Sandwich Structures & Materials*, 21(6), pp.1906-1929.
- [15] Al-Furjan, M.S.H., Safarpour, H., Habibi, M., Safarpour, M. and Tounsi, A., 2020. A comprehensive computational approach for nonlinear thermal instability of the electrically FG-GPLRC disk based on GDQ method. *Engineering with Computers*, pp.1-18.
- [16] Khiloun, M., Bousahla, A.A., Kaci, A., Bessaim, A., Tounsi, A. and Mahmoud, S.R., 2020. Analytical modeling of bending and vibration of thick advanced composite plates using a four-variable quasi 3D HSDT. *Engineering with Computers*, 36(3), pp.807-821.
- [17] Madan, R. and Bhowmick, S., 2020. A review on application of FGM fabricated using solid-state processes. *Advances in Materials and Processing Technologies*, 6(3), pp.608-619.
- [18] Madan, R., Saha, K. and Bhowmick, S., 2020. Limit speeds and stresses in power law functionally graded rotating disks. *Advances in materials Research*, 9(2), pp.115-131.
- [19] Pawar, S.P., Deshmukh, K.C. and Kedar, G.D., 2015. Thermal stresses in functionally graded hollow sphere due to non-uniform internal heat generation. *Applications and Applied Mathematics: An International Journal (AAM)*, 10(1), p.33.
- [20] Petrovic, R., Zivkovic, M., Topalović, M. and Slavkovic, R., 2015. Analytical, numerical and experimental stress assessment of the spherical tank with large volume. *Tehnicki Vjesnik*.